Semi-Analytical Electro-Thermal Modelling of a Photovoltaic Module for Evaluation of Spatial Temperature Distribution

Semi-analytical Electro-Thermal Modelling of a Photovoltaic Module for Evaluation of Spatial Temperature Distribution

Aldo Amodio
Scuola di Ingegneria
Università degli Studi della Basilicata
Potenza, Italy
aldo.amodio@studenti.unibas.it

Antonio D'Angola
Scuola di Ingegneria
Università degli Studi della Basilicata
Potenza, Italy
antonio.dangola@.unibas.it

Diana Enescu
Electronics, Telecommunications and Energy Department
Valahia University of Targoviste
Targoviste, Romania
Physical Thermodynamics Unit
INRiM, Torino, Italy
diana.enescu@valahia.ro, d.enescu@inrim.it

Antonio Ferraro
Scuola di Ingegneria
Università degli Studi della Basilicata
Potenza, Italy
antonio.ferraro@unibas.it

Gabriele Malgaroli
Dip. Energia "G. Ferraris"
Politecnico di Torino
Corso Duca Abruzzi 24, Torino, Italy
gabriele.malgaroli@polito.it

Filippo Spertino
Dip. Energia "G. Ferraris"
Politecnico di Torino
Corso Duca Abruzzi 24, Torino, Italy
filippo.spertino@polito.it

***Abstract*— The paper presents a two-dimensional thermal model coupled with the electrical model to investigate the performance of a PV module. An iterative procedure is implemented by calculating analytically the boundary conditions for each cell of the PV module placed in the environment, considering the effect of solar irradiance. The temperature distribution is then calculated in each cell using a numerical model where an accurate description of connections is included. The electric current can be calculated inside each cell, starting from cell temperature distributions. An updated source term, including Joule dissipation, is evaluated to enhance boundary conditions by applying the eigenfunctions expansion method. Stationary solutions are obtained at the end of the iterative procedure showing the effects of Joule dissipation on the module performance. The effects of environmental conditions, irradiance and ambient temperature on the PV module temperature are also investigated.**

***Keywords*— photovoltaic module, thermal model, electric model, spatial temperature distribution, semi-analytical analysis.**

I. INTRODUCTION

In recent years, the electric production by Renewable Energy Sources (RES) has increased to reduce the fossil fuels consumption and the environmental impact in terms of CO2 emissions by energy systems [1]. Among RES-based systems, PhotoVoltaic (PV) technology is the most diffused thanks to its reliability and low maintenance [2]. In this context, the assessment of most PV applications requires knowledge of the PV cell temperature and the solar irradiance incident on the PV module surface with reasonable accuracy [3]. This is due to the major influence of the cell temperature and incident solar irradiance on the PV module power generation and performance [4]. In particular, in the PV module design and operation, its performance is affected by the combined effect of weather variables (irradiance and external air temperature), as well as the local wind speed and its direction. The cell temperature considerably depends on the "plane-of-array" irradiance [5] and is mostly sensitive to wind velocity, while the impact of wind direction on the atmospheric temperature can be neglected. On the thermal side, the temperature variations impact the PV cells as other semiconductor devices [6]. The PV cells absorb up to about 80% of the incident solar irradiance and its amount incident on PV modules that is converted into electricity depends on their conversion efficiency [7]. Actually, PV cells convert a specific range of wavelengths for solar irradiance, while the other amount is converted into thermal energy [8], increasing the temperature of the PV cells up to 40°C above the ambient temperature [9]. On the electrical side, the electrical efficiency of PV cells decreases almost linearly as their operating temperature increases [10]. Hence, the maximum reduction of PV cell efficiency generally occurs when solar irradiance is the highest. Since the PV cell efficiency decreases with the operating temperature rise [11], when the PV cells are combined in a string, the PV cell that reaches the highest temperature becomes a bottleneck for the whole PV string [12]. Hence, keeping a homogeneous low-temperature distribution across the string is crucial for the best performance of the PV modules [7]. Therefore, knowing the temperature dependence on weather conditions represents a key asset to evaluate the PV performance [4].

Different factors negatively affect the performance of PV modules in outdoor applications. These factors, like soiling, low irradiance and high operating PV cell temperatures, contribute to the degradation of the PV cell lifetime and reduction of the PV conversion efficiency [13]. As a consequence of raising the operating temperature of the solar cells, two negative effects occur [14]:

- ✓ a reduction in the fill factor, i.e., the ratio of the actual maximum PV output power to the product between the open-circuit voltage V_{oc} and the short-circuit current I_{sc} [15];
- ✓ irreversible thermal damage due to long-time operating conditions at high PV cell temperatures [16].

The various correlations found in the literature express the PV cell temperature as a function of the weather variables and also include the parameters dependent on the material and system properties, such as plate absorbance, glazing-cover transmittance, etc. Furthermore, many correlations in the literature express the negative effect that the cell temperature rise has on the electrical efficiency of the PV module [17].

To estimate the PV cell temperature, different methods have been proposed, from empirical correlation to advanced thermal and electrical models. Empirical correlations are divided into implicit and explicit correlations. The implicit correlations require an iterative method for resolution, using the variables that depend on other correlated parameters [4], [17]. The typical implicit relation to determining the PV cell temperature starts from the Nominal Operating Cell Temperature (NOCT), the incident solar irradiance and the external air temperature [18]. The NOCT assesses the temperature dependence and represents the cell temperature in a module exposed at 45° South to an irradiance of 800 W/m^2 at an ambient temperature of 20 °C and wind speed at about 1m/s according to the IEC 61215 standards [19]. A comprehensive overview of the PV temperature simulation is described in [17]. Moreover, some models for the description of the correlations between the PV module temperatures, ambient temperature, solar irradiance , and wind have been proposed. The article [20] developed a statistical model based on principal component analysis and an analytical model for the temperature rating of PV modules from climatic data such as global irradiance, ambient temperature and wind speed. These models permit to simulate the PV module temperatures in transient conditions at periods and locations where the weather data are known. The paper [21] carried out a comparison of seven models validated with experimental data that estimated the PV module temperature using solar irradiance and various meteorological measurements. The article [22] compared seven models that express the cell temperature as a function of the meteorological data and the solar irradiance. The comparisons show that the residuals are described by a Gaussian distribution with the minimum half width at half maximum of about 2.2 °C. Implementation of a simple heat transfer model also resulted in similar uncertainties (about 2.1–2.2 °C). A more detailed approach is represented with various analytic thermal and electrical models.

The thermal modelling of the PV cell can be developed in steady-state conditions if the variables involved are constant over time or in transient conditions if the variables involved are time-dependent [23]. The thermal modelling advantage is to avoid the estimation of the parameters (*I-V* curves of the PV module) used in various electrical models, which the manufacturer does not provide. The electrical modelling of the PV cell involves a non-linear system of equations where unknown parameters appear. The manufacturers provide only the operational data for PV modules at Standard Test Conditions (STC), corresponding to irradiance equal to 1000 W/m^2, and cell temperature equal to 25°C [24]. Evaluating the PV module performance considers five models (radiation, optical, structural, thermal, and electrical models). These models involve the site where the PV modules are installed, the available meteorological data, the PV module physical characteristics and electrical data input, as shown in the block diagram of Fig. 1 [25]. The radiation and optical model calculate the absorbed solar energy that is sent as input to the thermal model to obtain the temperature field of the PV cells. The thermal model and electrical model are coupled to each other. Both the absorbed solar energy and the PV cell temperature field are inputs for the electrical model to get the electrical performance of the PV module.

Suggerimento di Filippo: la figura è poco leggibile, si può aumentare il carattere o ingrandirla?

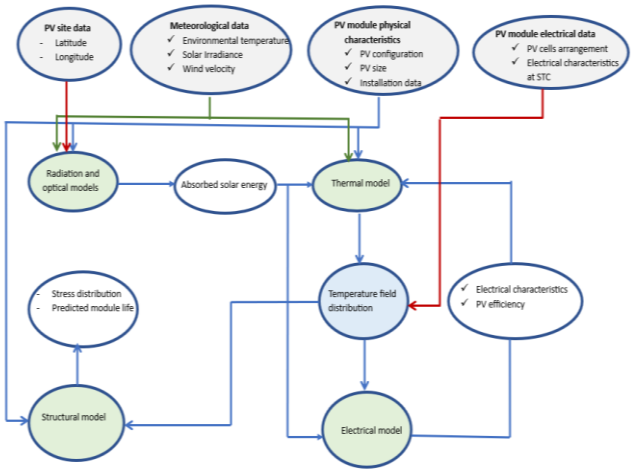

Fig. 1. Block diagram of the multiphysics modelling of a PV module (adapted from [25]).

The electrical efficiency of the PV module and the electrical characteristics are also sent back to the thermal model to update the amount of absorbed energy available for PV module heating. In addition, the temperature field distribution and the PV module physical characteristics are inputs for the structural model to evaluate the thermal stress developed in the PV module and assess the predicted module life and stress distribution.

This paper presents a two-dimensional (2D) thermal model coupled with the electrical model for a PV module. Moreover, the paper aims to present a mixed analytical and numerical procedure to evaluate the spatial distribution of the temperature, including Joule heating and the coupling between the thermal and electric models. The paper is organized as follows: section II recalls the theoretical background of the analytical method, and section III describes the steps of the implemented procedure.

Section IV presents the results for one silicon PV module under simulation, while Section V contains a discussion of the results and the conclusions.

II. Theoretical background of Analytical Solution

Suggerimento di Filippo: aggiungere qui la differenza tra soluzione numerica e analitica

This section describes the 2D analytical and numerical models in which the effect of the ambient temperature is combined with the Joule losses due to current transport through the ribbons that interconnect the neighbouring cells. The general heat conduction equation, known as the Fourier equation, in rectangular coordinates, is written as follows:

$$k \cdot \nabla^2 T + \dot{q}_{\mathrm{v}} = \rho \cdot c_{\mathrm{p}} \cdot \frac{\partial T}{\partial t} \qquad (1)$$

where T is the temperature, $\nabla^2 T = \frac{\partial^2 T}{\partial x^2} + \frac{\partial^2 T}{\partial y^2} + \frac{\partial^2 T}{\partial z^2}$ is the temperature Laplacian (denoting the spatial variables with *x*, *y* and *z*), $\dot{q}_{\mathrm{v}}$ is the internal heat generation source per unit volume, k is the thermal conductivity, ρ is the density, c_{p} is the specific heat capacity of the materials, and t is time.

Eq. (1) reduces to two particular forms under specified conditions:

- ✓ For steady-state conditions without heat generation source per unit volume, Eq. (1) can be simplified as follows:

$$k \cdot \nabla^2 T = 0 \qquad (2)$$

and is called Laplace equation.

- ✓ For steady-state conditions with heat generation source per unit volume, Eq. (1) can be simplified in the following way:

$$k \cdot \nabla^2 T + \dot{q}_{\mathrm{v}} = 0 \qquad (3)$$

and is called the Poisson equation [26].

In this paper, two-dimensional (2D) heat conduction is assumed, while the heat conduction in the *z* direction (i.e., the thickness of PV cells) is neglected. Heat transfer in the *z* direction, radiation and optical models are not considered in this model. In 2D, the Laplacian of the temperature for Eq. (1) is $\nabla^2 = \frac{\partial^2}{\partial \hat{x}^2} + \frac{\partial^2}{\partial \hat{y}^2}$.

The heat generation source per unit volume, $\dot{q}_{\mathrm{v}}$, can be considered as the sum of two contributions: the solar contribution due to the irradiance, $\dot{q}_{\mathrm{v,G}}$, and the Joule losses due to current transport through the ribbons, $\dot{q}_{\mathrm{v},\Omega} = R_V I^2$ where R_V is the electrical resistance per unit volume and I is the current flowing in the ribbons.

Eq. (3) can be expressed in a normalized form as follows:

$$\nabla^2 \theta(\hat{x}, \hat{y}) + \hat{\dot{q}}_{\mathrm{v}} = 0$$
$$\text{with } \hat{\dot{q}}_{\mathrm{v}} = \hat{\dot{q}}_{\mathrm{v,G}} + \hat{\dot{q}}_{\mathrm{v},\Omega} = \kappa \hat{G}[1 - \eta_{el}(\theta)] + \quad \mu \hat{I}^2 \qquad (4)$$

where $\theta(\hat{x}, \hat{y}) = \frac{T(\hat{x}, \hat{y}) - T_a}{T_a}$ represents the normalized temperature excess with respect to the ambient temperature T_a; $\kappa = \frac{L_R^2 G_{STC}}{h k T_a}$ and $\mu = \frac{L_R^2 P_{sc}}{k T_a}$ are dimensionless parameters with k is as thermal conductivity; L_R is the geometric mean and is equal to $\sqrt{L_x L_y}$ is a reference length; L_x, L_y and h are the width, the height and the thickness of the PV module, respectively; $P_{sc} = R_V I_{sc}^2$ is the volumetric power dissipation in the short circuit state (I=I_{sc}); $\hat{I} = \frac{I}{I_{sc}}$; $\eta_{el}(\theta)$ is the electrical efficiency, $\hat{G}$ is the normalized irradiance ($\hat{G} = \frac{G}{G_{STC}}$ with G_{STC} = 1000 Wm^{-2}) and finally $\hat{x} = \frac{x}{L_R}, \hat{y} = \frac{y}{L_R}$.

III. Description of the iterative procedure

The implemented iterative procedure consists of different stages:

- Step #1 - Determination of an initial tentative electric current I. In this step, an initial null current is imposed, and such a value will be updated at each iteration of the procedure.
- Step #2 - Evaluation of $\hat{\dot{q}}_{v,\Omega}$. In this step, the Joule losses per unit volume are estimated uniformly distributed inside the module according to Eq. (4).
- Step #3 – Analytical evaluation of the temperature profile. In this step, the normalized temperature profile $\theta(\hat{x}, \hat{y})$ and the boundary conditions are analytically evaluated inside the PV module (Subsection III.A).
- Step #4 – Numerical evaluation of the temperature field. In this step, the spatial distribution for temperature is numerically determined inside each cell (Section III.B).
- Step #5 – Evaluation of the current inside the PV module. In this step, starting from the maximum temperature inside each cell, the current circulating through the cells is analytically estimated (Section III.C) using a simplified electrical model. Steps from #2 to #5 are iteratively repeated until the steady-state solution is obtained.

In the following subsections, details on the analytic (step #3) and on the numerical calculations (step #4), as well as on the current estimation (step #5) in each cell, are discussed in depth.

A. Analytical solution of the temperature field in the PV module

The procedure applied in this paper consists in two phases. In the first stage, boundary conditions for each cell are calculated analytically in the isotropic plate placed in the environment. The heat source is the sum of the contribution of the

solar irradiance and the Joule heating, which is considered uniformly distributed inside each cell. The PV module under simulation consists of $nc_x \cdot nc_y$ cells. The analytical solution has been obtained by referring to the separation of variables method for the temperature excess $\theta(\hat{x},\hat{y})$ [27], which satisfies the thermal boundary conditions $\theta(\hat{x}=0=\delta,\hat{y}) = \theta(\hat{x},\hat{y}=0=\delta^{-1}) = 0$ and

$$\theta(\hat{x},\hat{y}) = X(\hat{x}) \cdot Y(\hat{y}) \tag{6}$$

Being δ is the adimensionless ratio between the width and the height of the module ($\sqrt{\frac{L_x}{L_y}}$). In the case of uniform source term, $\dot{\hat{q}}_{\mathrm{v}} = \dot{\hat{q}}_{\mathrm{v,G,0}} + \dot{\hat{q}}_{\mathrm{v,\Omega,0}}$, distributed over the PV module $\hat{x} \in [0,\delta] \cup \hat{y} \in [0,\delta^{-1}]$ (the Joule contribution is considered only on the $nc_x \cdot nc_y$ cell surfaces), the solution can be expressed as the superposition of the solar and Joule contributions:

$$\theta(\hat{x},\hat{y}) = \theta_G(\hat{x},\hat{y}) + \theta_\Omega(\hat{x},\hat{y}) \tag{7}$$

being

$$\theta_G(\hat{x},\hat{y}) = 4\dot{\hat{q}}_{\mathrm{v,G,0}} \sum_{n=1}^{\infty}\sum_{m=1}^{\infty} \frac{sin(\alpha_n\hat{x})\cdot sin(\beta_m\hat{y})}{(\alpha^2{}_n+\beta^2{}_m)\cdot\alpha_n\cdot\beta_m} \cdot [cos(\alpha_n\delta)-1]\cdot[cos(\beta_m\delta^{-1})-1] \tag{8}$$

and

$$\theta_\Omega(\hat{x},\hat{y}) = 4\dot{\hat{q}}_{\mathrm{v,G,\Omega}} \sum_{n=1}^{\infty}\sum_{m=1}^{\infty} \frac{sin(\alpha_n\hat{x})\cdot sin(\beta_m\hat{y})}{(\alpha^2{}_n+\beta^2{}_m)\cdot\alpha_n\cdot\beta_m} \sum_{l=1}^{nc_x-1}\sum_{v=1}^{nc_y-1} [cos(\alpha_n\cdot\hat{x}_{l+1}) - cos(\alpha_n\cdot\hat{x}_l)]\cdot [cos(\beta_m\cdot\hat{y}_{v+1}) - cos(\beta_m\cdot\hat{y}_v)] \tag{9}$$

where $\hat{x} \in [\hat{x}_l,\hat{x}_{l+1}] \cup \hat{y} \in [\hat{y}_v,\hat{y}_{v+1}]$ represents the domain of the cell (l,v) and $\alpha_n = \frac{n\pi}{\delta}, \beta_m = \frac{m\pi}{\delta^{-1}}$ are the eigenvalues.

The boundary conditions can be calculated for each cell (step #3) by using Eqs. (7-9) Furthermore the cell is individually investigated in detail taking into account the electrical connections for the evaluation of the Joule heating and its location inside the module applying the boundary conditions. In Fig. 3, a scheme of the most important steps, i.e., steps #3 and #4, is reported. Starting from the analytical solution, which is evaluated by assuming a uniform source term inside the cells, approximate boundary conditions can be obtained (step #3). Then, an accurate evaluation of the temperature distribution inside the cell is numerically obtained by considering a precise modelling of the Joule losses due to electrical connections (step #4).

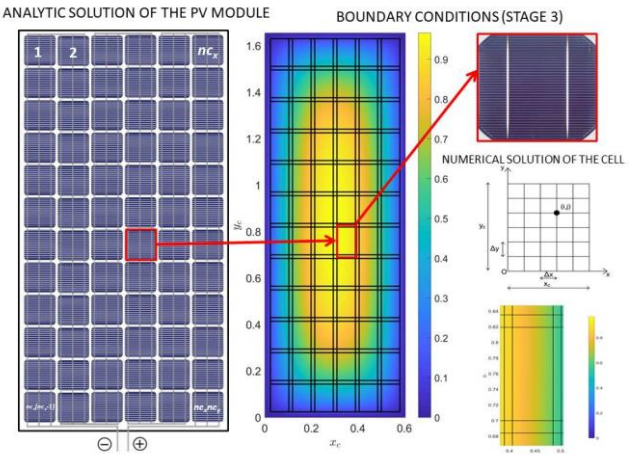

Fig. 3. Description of the numerical procedure: analytical evaluation of the boundary conditions (step # 3) and numerical calculation of the temperature distribution inside the cell (step #4).
Suggerimento di Filippo: Si può spostare sotto l'immagine "analitica" la parte relativa a quella numerica perchè poco leggibile

In Fig. 4, an example of boundary conditions implemented in the numerical solution of the cells is reported. The PV module under simulation contains 72 cells: results of analytical solution for cell #59 are presented for up/left (full line) and bottom/right (dashed line) edges of the cell. Analytic boundary conditions are reported for $T_a = 36^o$ C (Fig 4a) and 20^o C (Fig. 4b) (controllare che le T, che ho esplicitato qui nel testo, siano coerenti con la figura 4) in the case of $\kappa = 26.96$, $\mu = 2.16$ and $\hat{G} = 1$.

B. Numerical solution of the temperature field in each PV cell

The cell temperature distribution in each PV cell is calculated using a separate centred finite-difference numerical approximation in which a detailed description of the components is included. In fact, by using a rectangular grid, composed by N_xN_y cells with grid spacing $\Delta x = \frac{x_c}{N_x}, \Delta y = \frac{y_c}{N_y}$, the discretized heat equation (4) for the node (i,j) becomes:

$$\frac{\theta_{i+1,j}+\theta_{i-1,j}-2\theta_{i,j}}{\Delta x^2} + \frac{\theta_{i,j+1}+\theta_{i,j-1}-2\theta_{i,j}}{\Delta y^2} = -\dot{\hat{q}}_{v,i,j} \tag{10}$$

Analytic boundary conditions, given by Eqs. (8) and (9), are applied to equations involving boundary nodes and heat sources, iteratively updated and given by Eq. (4), are included. Finally, by defining a sparse pentadiagonal matrix with principal

diagonal: $-\frac{2}{\Delta x^2}-\frac{2}{\Delta y^2}$, upper and lower diagonals (offset ±1): $-\frac{2}{\Delta y^2}$, offdiagonals (offset ± N_y-1): $-\frac{2}{\Delta x^2}$, heat equation is solved by means of a system of linear equations. In the simulations a numerical grid constituted by $N_x = N_y = 80$ grid cells has been considered. The advantage of this semi-analytic procedure is calculating the behaviour of a single cell of the PV module by decoupling from the other cells by the iterative approach. In fact, by adopting the iterative technique, boundary conditions are evaluated at each step and a steady-state solution can be obtained.

C. Evaluation of the current inside the PV module

At the end of each iteration (step #5), the cell temperature distribution inside each cell is known and the average or the maximum value can be used to evaluate the electric current and the electrical efficiency at temperature T according to the following equations [28]:

$$I(T) = I_{STC} \cdot [1 + \alpha \cdot (T - T_{STC})] \qquad (11)$$

and

$$\eta_{el}(T) = \eta_{el,STC} \cdot \left[1 + \gamma_P \cdot (T - T_{STC})\right]$$
$$\text{with } \eta_{el}(T) = P_{el}(G,T)/(G \cdot A) \qquad (12)$$

where $\eta_{el,STC}$ and I_{STC} are the efficiency and the electric current at Standard Test Conditions (STC), P_{el} is the PV power, A is the surface of the PV module or cell, α and γ_P are the thermal coefficients for short-circuit current and power, respectively.

Ho inserito (a) e (b) nella figura 4: si potrebbero mettere nel grafico originale?

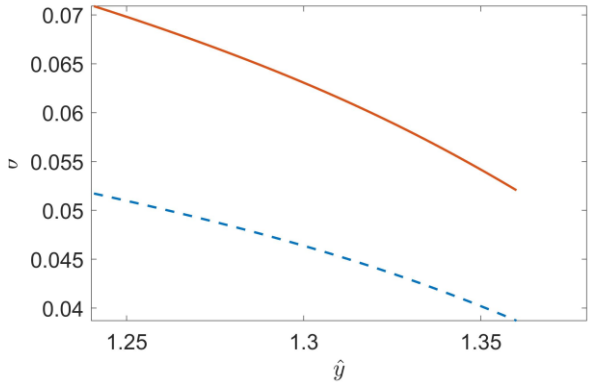

(a)

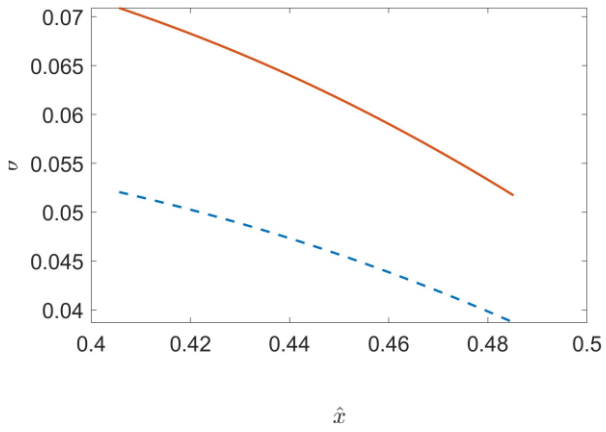

(b)

Fig. 4. Analytic boundary conditions for the cell #59.

IV. Results

Numerical simulations have been carried out to investigate the effects of environmental conditions, such as irradiance and ambient temperature on the maximum temperature of the PV module. A silicon PV module has been considered with the following parameters $\alpha = 0.03\ \%/°C$, $\gamma_P = -0.5\ \%/°C$, $\eta_{el,STC} = 20\%$, $I_{STC} = 11.05$ A, $NOCT = 45\ ^oC$. In the simulations, the parameters κ and μ ranged in the following intervals, $\kappa \in [2.57,2.95]$ and $\mu \in [0.02,0.24]$, according to ambient temperature T_a. In Fig. 5, the maximum values of θ ($\theta(\hat{x},\hat{y}) = \frac{T(\hat{x},\hat{y})-T_a}{T_a}$) have been reported as a function of the ambient temperature and of the irradiance. Results show the dependence of the normalized excess temperature θ on the irradiance. Absolute cell temperature also depends on the ambient temperature, increasing with it. In fact, maximum cell temperatures have been reported in Fig. 6a as a function of irradiance for different values of ambient temperature (squares for

T_a = -5 °C, diamonds for T_a = 20 °C, crosses for T_a = 35 °C), while as a function of the ambient temperature (Fig. 6b) for different values of the irradiance (stars for $\hat{G} = 0.1$, circles for $\hat{G} = 0.3$, squares for $\hat{G} = 0.7$, crosses for $\hat{G} = 1$). Numerical results have been compared with the empirical formula which states a linear dependence between the solar irradiance and the difference between the cell temperature in NOCT conditions and ambient temperature [29]:

$$T = T_a + \frac{NOCT - 20}{800} \cdot G \qquad (13)$$

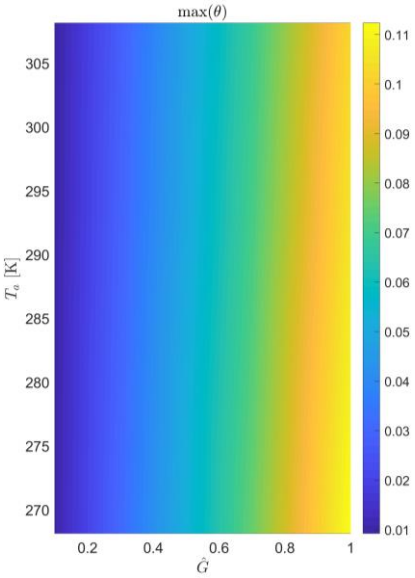

Fig. 5. Maximum θ values as a function of irradiance $\hat{G}$ and ambient temperature T_a.

Results reported in Fig. 6 show the excellent agreement between the maximum values of the cell temperature calculated numerically (T_{num}, lines) and the values obtained with the empirical formula (13) (T_{NOCT}, markers). In particular, the deviations $(T_{num} - T_{NOCT})/T_{NOCT}$ are in the range -0.7% — +0.1%. Such comparisons have been made with the maximum value of the cell temperature but the semi-analytic model calculates the spatial temperature distributions which depend on the chosen boundary conditions. As an example, Figure 7 shows the spatial temperature distribution in the case of $T_a = 35^o\mathrm{C}$ and $\hat{G} = 1$. In the simulations $\kappa = 2.57, \mu = 0.21$. Analytic boundary conditions are calculated analytically by recurring to the eigenfunction expansion method. In the case of a uniform source, the number of eigenfunctions used in Eqs. (8) and (9) is lower than 10 and the implementation is relatively fast. Spatial distributions of the excess temperature is then calculated for each cell taking into account the Joule dissipation and the electric current circulating in the module is identified.

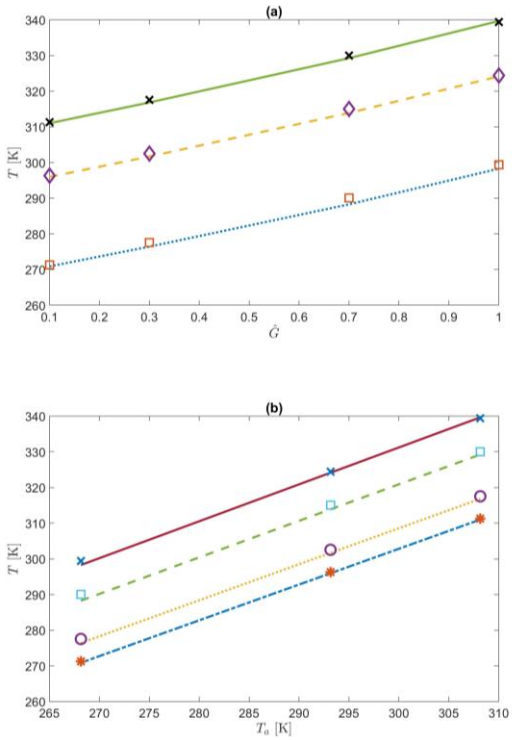

Fig. 6. Maximum cell temperature as a function of the irradiance $\hat{G}$ and ambient temperature T_a.

V. Discussion and Conclusions

In this paper, a 2D coupled thermal and electrical model has been presented to investigate the performance of a PV module. In this work, radiation and optical models are not included, and the heat conduction in the z direction is neglected. In particular, an iterative procedure is implemented to determine analytically the temperature profile of the module, as well as the boundary conditions for each cell exposed to sunlight. Then, in each cell, the spatial temperature distribution is calculated using a numerical model in which an accurate description of electric connections and Joule heating are included. Stationary solutions are obtained at the end of the iterative procedure in order to investigate the effects of weather conditions, irradiance and ambient temperature, on the PV module temperature. The procedure is applied to one silicon PV module with the following parameters parameters: $\alpha = 0.03\ \%/°C$, $\gamma_P = -0.5\,\%/°C$, $\eta_{el,STC} = 20\%$, $I_{STC} = 11.05\,\mathrm{A}$, $T_{NOCT} = 45\ ^oC$. Numerical results have been compared with the empirical formula based on NOCT to evaluate the module temperature. In particular, the relative deviations between numerical simulations and the empirical equation confirm the accuracy of the proposed procedure, ranging between -0.7% and +0.1%. By means of this study thermal effect on the performance of PV model can be investigated and direct applications could be the degradation of the modules and the effects produced by shadows. In future works, the semi-analytic model will be improved to include heat transfer in z direction and an accurate description of the optical model. In addition, the electrical model used to estimate the PV current starting from the knowledge of cells' temperature will be replaced by the well-known single diode model to improve the accuracy of the procedure. Such a model is based on a transcendental implicit equation, which requires additional computational efforts, but it permits to find more accurate solutions with respect to the electrical model used in this work.

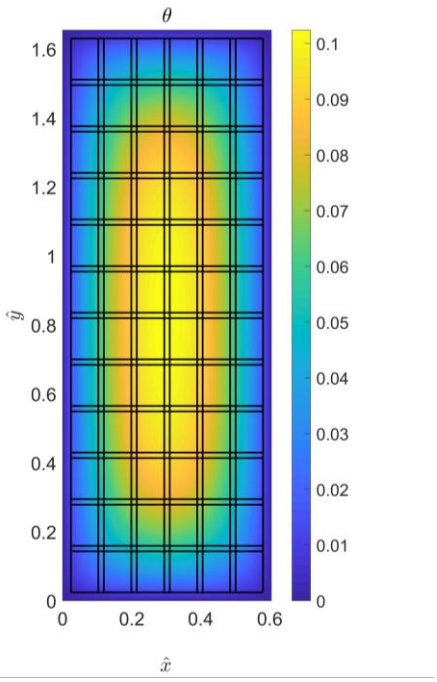

Fig. 7. Spatial distribution of the normalized excess temperature θ.

References

[1] S. Materi , A. D'Angol, D. Enescu, and P. Renna, "Reducing energy costs and CO_2 emissions by production system energy flexibility through the integration of renewable energy", J. Prod. Eng.,vol. 15(5)pp. 667 – 681, , 2021.

[2] F. Bizzarri, S. Nitti, G. Malgaroli, "The use of drones in the maintenance of photovoltaic fields," (2019) E3S Web of Conferences.

[3] A. Ciocia, P. Di Leo, S. Fichera, F. Giordano, G. Malgaroli, F. Spertino, "A novel procedure to adjust the equivalent circuit parameters of photovoltaic modules under shading," 2020 International Symposium on Power Electronics, Electrical Drives, Automation and Motion, SPEEDAM 2020, art. no. 9161878, pp. 711 - 715, DOI: 10.1109/SPEEDAM48782.2020.9161878.

[4] P. Bevilacqua, S. Perrella, R. Bruno, N. Arcuri, "An accurate thermal model for the PV electric generation prediction: long-term validation in different climatic conditions, " Renewable Energy, vol. 163, pp. 1092–1112, 2021.

[5] E. Skoplaki, A.G. Boudouvis, J.A. Palyvos, " A simple correlation for the operating temperature of photovoltaic modules of arbitrary mounting, " Solar Energy Materials and Solar Cells, vol. 92 (11), pp. 1393-1402, 2008.

[6] T. Kim, D. Lee; Y. Ko; K. Hwang; N. Kim, "Thermal Analysis and Design Optimization of Photovoltaic Module for Improved Heat Dissipation From Photovoltaic Module," IEEE Journal of Photovoltaics, vol.12 (5), pp.1198–1204, 2022.

[7] A. Makki, S. Omer, H. Sabir, " Advancements in hybrid photovoltaic systems for enhanced solar cells performance," Renew. Sustain. Energy Rev. vol. 41, pp. 658–684, 2015.

[8] F. Spertino, A. D'Angola, D. Enescu, P. Di Leo, G. V. Fracastoro, and R. Zaffina. "Thermal-electrical model for energy estimation of a water cooled photovoltaic module," Sol Energy, vol. 133, pp. 119–140,, 2016.

[9] A. Luque, S. Hegedus, " Handbook of photovoltaic science and engineering," 2nd ed. West Sussex: John Wiley&Sons, 2011.

[10] B.J. Brinkworth, B. M. Cross, R.H. Marshall, H. Yang, "Thermal regulation of photovoltaic cladding, " Solar Energy, vol.61, pp. 169–178, 1997.

[11] A. D'Angola, R,. Zaffina D. Enescu, P. Di Leo, G.V. Fracastoro, and F. Spertino "Best compromise of net power gain in a cooled photovoltaic system. In: 2016 51st International Universities Power Engineering Conference (UPEC), pp 1–6., 2016.

[12] G. Antonetto, M.Morciano, M. Alberghini, G. Malgaroli, A. Ciocia, L. Bergamasco, F. Spertino, M. Fasano, “Synergistic freshwater and electricity production using passive membrane distillation and waste heat recovered from camouflaged photovoltaic modules,”(2021) Journal of Cleaner Production, 318, art. no. 128464, DOI: 10.1016/j.jclepro.2021.128464.
[13] S. Chatterjee, G.B. Tamizh Mani, “A PV arrays: side-by-side comparison with and without fan cooling. In: IEEE photovoltaic specialists conference (PVSC) 2011, vol 7, pp537–542, 2011.
[14] Y. Gao, D. Wu, Z. Dai, C. Wang, B. Chen, X. Zhang, “A comprehensive review of the current status, developments, and outlooks of heat pipe photovoltaic and photovoltaic/thermal systems,” Renewable Energy, vol. 207, pp. 539-574, 2023.
[15] S. Sargunanathan, A. Elango, S.T. Mohideen, “Performance enhancement of solar photovoltaic cells using effective cooling methods: a review,” Renew. Sustain. Energy Rev., vol. 64, pp. 382–393, 2016.
[16] Y. Wang, Y. Gao, Q. Huang, G. Hu, L. Zhou, “Experimental study of active phase change cooling technique based on porous media for photovoltaic thermal management and efficiency enhancement,” Energy Convers. Manag., vol. 199, 111990, 2019.
[17] E. Skoplaki, J.A. Palyvos, “Operating temperature of photovoltaic modules: a survey of pertinent correlations,” Renew. Energy, vol.34 (1), pp.23-29, 2009.
[18] M.C. Alonso García, J.L. Balenzategui, “Estimation of photovoltaic module yearly temperature and performance based on Nominal Operation Cell Temperature calculations,” Renew. Energy, vol.29 (12), pp. 1997-2010, 2004.
[19] IEC61215 ed.2 (Crystalline Silicon Thin-Film Terrestrial Photovoltaic (PV) Modules Design Qualification and Type Approval) and IEC 61646 ed.2 (Thin-Film Terrestrial Photovoltaic (PV) Modules—Design Qualification and Type Approval).
[20] M. Koehl, M. Heck, S. Wiesmeier, J. Wirth, “ Modeling of the nominal operating cell temperature based on outdoor weathering,” Sol. Energy Mater. Sol. Cells, vol. 95 (7), pp. 1638-1646, 2011.
[21] M. Mattei, G. Notton, C. Cristofari, M. Muselli, P. Poggi, “ Calculation of the polycrystalline PV module temperature using a simple method of energy balance,” Renew. Energy, vol.21 (4), pp. 553-567, 2006.
[22] F. Mavromatakis, E. Kavoussanaki, F. Vignola, Y. Franghiadakis, “ Measuring and estimating the temperature of photovoltaic modules,” Sol. Energy, vol.110, pp. 656-666, 2014.
[23] N. Aoun, N. Bailek, “Evaluation of mathematical methods to characterize the electrical parameters of photovoltaic modules,” Energy Convers. Manag., vol.193, pp. 25-38, 2019.
[24] W. De Soto, S.A. Klein, W.A. Beckman, Erratum to “Improvement and validation of a model for photovoltaic array performance”, Sol. Energy vol. 80, pp. 78-88, 2006.
[25] M.U. Siddiqui, O. K. Siddiqui, A. B.S. Alquaity, H. Ali, A.F.M. Arif, S.M. Zubair, “A comprehensive review on multi-physics modeling of photovoltaic modules,” Energy Convers. Manag.,, vol. 258,115414, 2022.
[26] Y.A. Çengel J.M. Cimbala, and Ghajar A.J. Fundamentals of Thermal –Fluid Sciences . Sixth Edition, McGraw−Hill Companies, NY, USA, 2022.
[27] V. Arpaci, “Conduction Heat Transfer, Addison-Wesley,”New York, NY, 1966.
[28] A. D’Angola, D. Enescu, M. Mecca, A. Ciocia, P. Di Leo, G.V. Fracastoro, and F. Spertino “Theoretical and numerical study of a photovoltaic system with active fluid cooling by a fully-coupled 3D thermal and electric model,“ Energies vol.13, pp.852, 2020.
[29] ASTM, Standard test methods for electrical performance of non concentrator terrestrial photovoltaic modules ad arrays using reference cells. Standard E1036, The American Society for Testing and Materials, West Conshohocken, PA, USA, 1998.